Inhibition of Jagged-mediated Notch signaling disrupts zebrafish biliary development and generates multi-organ defects compatible with an Alagille syndrome phenocopy

Kristin Lorent[1], Sang-Yeob Yeo[2], Takaya Oda[3,*], Settara Chandrasekharappa[3], Ajay Chitnis[2], Randolph P. Matthews[4] and Michael Pack[1,5,†]

[1]Department of Medicine, University of Pennsylvania School of Medicine, 421 Curie Boulevard, Philadelphia, PA 19104-6058, USA
[2]Laboratory of Molecular Genetics, NICHD, NIH, 31 Center Drive, 9000 Rockville Pike, Bethesda, MD 20892-2425, USA
[3]Genome Technology Branch, NHGRI, NIH, 49 Convent Drive, 9000 Rockville Pike, Bethesda, MD 20892-2152, USA
[4]Division of Gastroenterology and Nutrition, Children's Hospital of Philadelphia, 34th Street and Civic Center Boulevard, Philadelphia, PA 19104, USA
[5]Department of Cell and Developmental Biology, University of Pennsylvania School of Medicine, Philadelphia, PA 19104-6058, USA

*Present address: Department of Molecular Biology, University of the Ryukyus, Faculty of Medicine, Okinawa 903-0215, Japan
†Author for correspondence (e-mail: mpack@mail.med.upenn.edu)

Accepted 20 August 2004

Development 131, 5753-5766
Published by The Company of Biologists 2004
doi:10.1242/dev.01411

Summary

The Alagille Syndrome (AGS) is a heritable disorder affecting the liver and other organs. Causative dominant mutations in human Jagged 1 have been identified in most AGS patients. Related organ defects occur in mice that carry *jagged 1* and *notch 2* mutations. Multiple *jagged* and *notch* genes are expressed in the developing zebrafish liver. Compound *jagged* and *notch* gene knockdowns alter zebrafish biliary, kidney, pancreatic, cardiac and craniofacial development in a manner compatible with an AGS phenocopy. These data confirm an evolutionarily conserved role for Notch signaling in vertebrate liver development, and support the zebrafish as a model system for diseases of the human biliary system.

Key words: Zebrafish, Notch, Jagged, Alagille Syndrome, Bile Duct, Biliary Development

Introduction

The synthesis and secretion of bile is one of the cardinal functions of the vertebrate liver. Bile is required for the absorption of dietary lipids and fat-soluble nutrients, as well as for the excretion of lipid-soluble compounds such as bilirubin, cholesterol and drugs. Bile is synthesized by hepatocytes, the principal liver cell type, and is excreted into the biliary system through a specialized portion of the hepatocyte membrane, the canaliculus. Within the biliary system, bile is modified prior to transport to the gallbladder and intestine.

Heritable defects of the intrahepatic biliary system are an important cause of pediatric liver disease. These disorders arise from either developmental defects or defects that injure cholangiocytes, the cells that comprise the bile ducts (McKiernan, 2002). Cholangiocyte injury may be immune mediated, or may arise from metabolic defects that alter the composition of bile. Alagille Syndrome (AGS) is a multisystem developmental disorder that affects the liver, heart and craniofacium, but it can also impair the function of the kidney, pancreas, nervous system and other organs (Piccoli and Witzleben, 2000). Liver disease in individuals with AGS arises from a relative lack of bile ducts. Bile duct paucity reduces bile flow (cholestasis) and can lead to liver fibrosis that requires liver transplantation.

Haploinsufficiency for Jagged 1 has been shown to be responsible for the majority of AGS cases (Li et al., 1997; Oda et al., 1997; Piccoli and Spinner, 2001; Spinner et al., 2001). Mice that are heterozygous carriers of a *jagged 1* null allele and a hypomorphic *notch 2* allele have liver, kidney and cardiac defects resembling those seen in AGS (McCright et al., 2002). Mice homozygous for the hypomorphic allele of *notch 2* have liver, kidney, heart and eye vasculature defects compatible with an AGS phenocopy (McCright et al., 2001; McCright et al., 2002). These data reveal a conserved role for Notch signaling in the development of the mammalian biliary system, heart, and other organs.

During mammalian organogenesis Notch signaling regulates cell fate decisions through one of two principal mechanisms. In the nervous system, Notch-mediated lateral inhibition defines neural precursors within a field of equipotent progenitors (Lewis, 1998). During vascular development and in other settings, Notch may function in an inductive manner (Lawson et al., 2001). How Notch signaling regulates mammalian biliary development is not known. Mammalian cholangiocytes and hepatocytes appear to develop from a common precursor, the hepatoblast (reviewed by Lemaigre, 2003; Rogler, 1997; Shiojiri, 1984; Shiojiri et al., 2001). Expression of *jagged 1*, and *notch 2* and *notch 3* genes within portal vein endothelia and mesenchyme, and adjacent hepatoblasts is compatible with an inductive mechanism (Loomes et al., 2002; Louis et al., 1999; McCright et al., 2002).

In this model, hepatoblasts that receive the Notch signal form biliary epithelia. Subsequently, these cells arrange to form tubules that remodel and become incorporated into the portal tract as interlobular bile ducts, the principal branch of the intrahepatic biliary tree (reviewed by Lemaigre, 2003).

The biliary system of lower vertebrates functions similarly to that of mammals. However, relatively little is known about the molecular regulation of biliary development in these organisms. Given the suitability of the zebrafish for genetic and embryological analyses, such studies may be relevant to human liver diseases. In this work, we identify a role for Notch signaling in zebrafish biliary development, and also show that the perturbation of Notch signaling produces kidney, craniofacial, cardiac and pancreatic defects compatible with an AGS phenocopy. Furthermore, we present data supporting a model in which the Notch signal promotes the development of biliary epithelial cells (cholangiocytes) from a bipotential precursor, the hepatoblast, as suggested by classical models. These data support the utility of the zebrafish as a model of human liver diseases, and identify conserved mechanisms that regulate development of the liver and other vertebrate organs.

Materials and methods

Fish maintenance and breeding

Fish maintenance and matings were performed as described (Pack et al., 1996). For all experiments TLF strain wild-type fish were used.

Histology

Embryos, larvae and adult liver were fixed in 4% paraformaldehyde/2% glutaraldehyde at 4°C overnight. Washed specimens were embedded in glycol methacrylate (JB-4 Plus, Polysciences). Histological sections were prepared as described (Pack et al., 1996).

RNA in situ hybridization

Whole-mount RNA in situ hybridization was performed as previously described (Pack et al., 1996). Anti-sense probes were transcribed from cDNAs for zebrafish *jagged 1*, *jagged 2*, *jagged 3*, *notch 1a*, *notch 1b*, *notch 2* and *notch 5*.

Immunohistochemistry

Primary antibodies used were: mouse monoclonal anti-human cytokeratin 18 antibody (Ks 18.04), 1:500 (Maine Biotechnology Services), and rabbit anti-bovine cytokeratin, 1:500 (suitable for wide spectrum screening; DAKO), used interchangeably; rabbit anti-human mdr (P-glycoprotein, Ab-1), 1:200 (Oncogene), rabbit anti-mouse Bsep 90365, 1:500 (gift from Richard M. Green), rabbit anti-human Mdr-1 (H-241) (Santa Cruz Biotechnology), rabbit anti-bovine carboxypeptidase, 1:300 (Rockland). Secondary antibodies were: Alexa Fluor 488-conjugated goat anti-mouse IgG, Alexa Fluor 488-conjugated goat anti-rabbit IgG, Alexa Fluor 568-conjugated goat anti-rabbit IgG (Molecular Probes). All secondary antibodies were used at a 1:600 dilution.

Embryos, larvae and adult liver were fixed for two hours at room temperature in 4% paraformaldehyde for P-glycoprotein and Bsep antibody staining, or in 4:1 (v/v) methanol:DMSO for cytokeratin antibody staining. For P-glycoprotein and Bsep staining, embryos, larvae and adult liver were pre-treated with 0.1% collagenase (Sigma) in PBS for 35 minutes at room temperature. Incubation in primary antibody was overnight at 4°C. Secondary antibody incubations were for 4 hours at room temperature, or overnight at 4°C. Some immunostained specimens were processed for histology as described above. A Zeiss LSM 510 confocal microscope was used for all analyses.

Morpholino injections

Morpholinos (Gene Tools, LLC) were stored at a stock concentration of 2 mM at –20°C. *jagged 1* morpholino (5′-cggtttgtctgtctgtgtctgtc-3′) was injected at a 1:40 dilution separately, and a 1:60 dilution in combination with other morpholinos. *jagged 2* (5′-tcctgatacaattccacat-gccgcc-3′), *jagged 3* (5′-ctgaactccgtcgcagaatcatgcc-3′) (Kim and Chitnis, unpublished), *notch 1a* (5′-gaaacggttcataactccgcctcgg-3′), *notch 1b* (5′-ctctccccattcattctggttgtcg-3′), *notch 2* (5′-aggtgaacact-tacttcatgccaaa-3′) and *notch 5* (5′-atatccaaaggctgtaattccccat-3′) morpholinos were injected at a 1:5 dilution separately, or a 1:10 dilution when combined. For *notch 2*, we used an exon-intron morpholino, for all other genes a morpholino against the 5′ end was injected. Injection of the *notch 2* morpholino generated a novel transcript with a 56-bp insertion upstream of the ankyrin repeat domain, at the end of exon 7 of the *notch 2* gene. This cDNA is predicted to generate a premature stop codon after the last exon 7 codon, thus deleting the entire ankyrin repeat domain.

In vitro translation

Jagged 1, 2 and 3 proteins were synthesized in the presence or absence of morpholinos for *jagged 1*, *2* or *3*, using TNT-coupled reticulocyte lysates systems (Promega). CS2+ *jagged 1*, *2* and *3* plasmids purified by Qiagen Plasmid Midi kit (0.5 μg/reaction) were used for the TNT reaction carried out at 30°C for 90 minutes in a total volume of 20 μl. Sp6 RNA polymerase, trans-[^{35}S] methionine label (20 μC), was added to the TNT reactions. After the translation reaction was complete, reaction mixtures were resolved on 4%-20% SDS-polyacrylamide gels (Invitrogen). The dried gel was exposed to X-ray film (Kodak).

Results

Zebrafish liver anatomy: lobular versus tubular architecture of the mammalian and teleost liver

The functional unit of the mammalian liver is commonly referred to as the liver lobule (Wanless, 2002). A lobule consists of plates of bilayered hepatocytes surrounded by portal tracts (Fig. 1A). The biliary system arises within the liver lobule. Bile enters the biliary tree through the canaliculus, a specialized region of the apical hepatocyte membrane that is contiguous with the smallest biliary radicles, the canals of Hering. The canals of Hering are hybrid tubules comprised of cholangiocytes fused to the terminal region of the canaliculus. Canals of Hering join interlobular bile ducts within the portal tracts. These ducts join larger ducts within the liver that carry bile to the common bile duct, gallbladder and, ultimately, the intestine.

Histological architecture of the teleost liver differs considerably from that of mammals (Fig. 1B) (reviewed by Hinton and Couch, 1998). In teleosts, portal veins, hepatic arteries and large bile ducts appear to be randomly distributed within the hepatic parenchyma, rather than in portal tracts. In addition, hepatocytes are arranged as tubules that surround small biliary ducts, rather than as bilayered plates. With this acinar or glandular arrangement, hepatocyte canaliculi are contiguous with ductular cells that are located within the hepatocyte tubule. Bile secreted by teleost hepatocytes enters the centrally located ducts that form a network of biliary channels. Ultimately, these small ducts, which are not apparent on routine histological sections, join large ducts that carry bile to the extrahepatic biliary system and the gallbladder. These larger ducts can be identified histologically.

Zebrafish liver architecture is comparable to this teleost

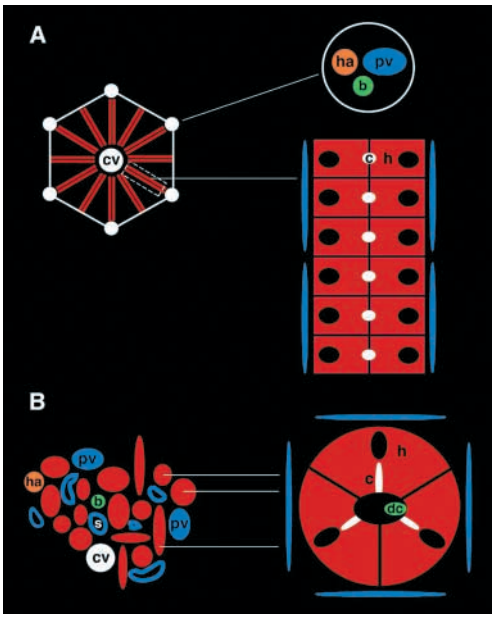

Fig. 1. Mammalian and teleost liver architecture. (A) Schematic representation of the mammalian liver lobule. Portal tracts (white circles) surround bilayered hepatocyte plates (h). Each portal tract contains a portal vein radicle (pv), a hepatic artery radicle (ha), and 1 or 2 interlobular bile ducts (b). Apical bicellular canaliculi (c) are located between adjacent hepatocytes. Fenestrated sinusoidal endothelial cells that line the basal hepatocyte membrane (depicted in blue) allow uptake and transport of proteins and other macromolecules. Blood enters the liver lobule through pv and ha radicles, and flows through sinusoidal channels lined by basal endothelial cells towards the central vein (cv), the proximal branch of the hepatic venous system. (B) Schematic representation of the teleost tubular liver. Portal vein radicles (pv), hepatic artery radicles (ha) and bile ducts are not grouped together in portal tracts. Note, portal venous and hepatic venous (cv) radicles are indistinguishable, although they are depicted in different colors for this schematic. Hepatocytes are arranged in tubules rather than in bilayered plates, and are surrounded by fenestrated endothelia. Longitudinal, transverse and oblique sections of hepatocyte tubules are present in histological sections, but are often difficult to appreciate. Small bile ducts (ducts) reside within hepatocyte tubules. In this schematic, a bile duct composed of a single biliary epithelial cell (dc) anastomoses with three hepatocyte canaliculi (c). Unicellular canaliculi of *cyprinid* fish are tubular invaginations of the hepatocyte membrane that extend to a perinuclear location. Note, biliary-arteriolar tracts (not shown) are described for some fish. [Adapted from Hinton and Couch (Hinton and Couch, 1998).]

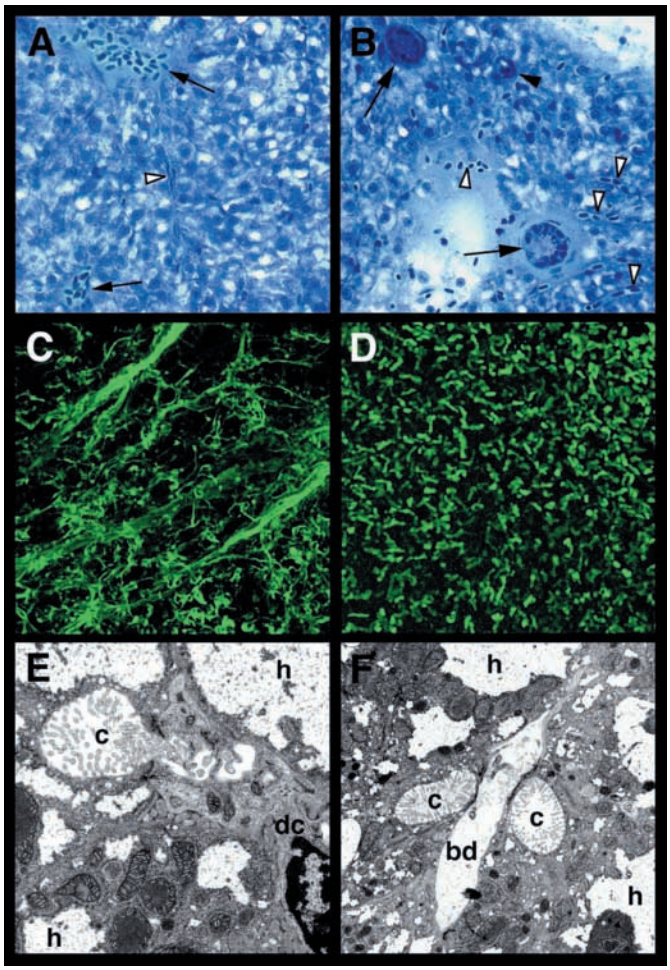

Fig. 2. Zebrafish adult liver. (A,B) Histological sections from an adult male liver. In A, two intrahepatic veins are visible (arrows). Identification of either vein as a portal or hepatic venous radicle is not possible. Sinusoidal channels containing nucleated red blood cells are visible between hepatocytes, most prominently in B (white arrowheads). Contiguous sinusoids linking adjacent venous structures are not seen. Large bile ducts are also visible in cross section (arrows in B), as is a smaller biliary radicle (arrowhead). Such ducts are infrequently seen in the liver periphery. (C,D) Confocal projections of adult liver samples processed for immunohistochemistry (IHC) using anti-human cytokeratin 18 (C) and anti-human P-glycoprotein (D) antibodies. Note branching anastomotic network of bile ducts, and tubular canaliculi described in other teleosts. (E,F) Transmission electron micrographs of adult liver. In each, ductular cells anastomose with hepatocyte canaliculi that have prominent microvilli. Multiple canaliculi converging on a single bile duct are evident (F). bd, bile duct; c, canaliculus; dc, ductular cell; h, hepatocyte.

model. Histological sections of adult liver show dispersed vascular elements within a field of seemingly unorganized hepatocytes (Fig. 2A,B). As described for other teleosts (Hinton and Couch, 1998), portal vein and hepatic vein branches are indistinguishable from one another. In addition, the sinusoidal channels that connect these venous radicles cannot be identified, and bile ducts are infrequently seen beyond the liver hilum. These histological features are comparable to the liver histology of other teleost fish and suggest that zebrafish hepatocytes are also arranged in tubules encasing the biliary tract.

Ultrastructural analyses and immunohistochemical studies support this architectural model. Although only a small number of large bile ducts are seen in histological sections, numerous small bile ducts are identified in adult tissue samples processed for cytokeratin immunohistochemistry (IHC) (Fig. 2C). Transmission electron micrographs (TEM) revealed that the cholangiocytes of these small ducts anastomose with canaliculi from several adjacent hepatocytes (Fig. 2E,F). These and other architectural features (Fig. 2D) of the zebrafish liver are similar to what has been reported in other teleost fish, and lead us to conclude that the tubular liver architecture described for these

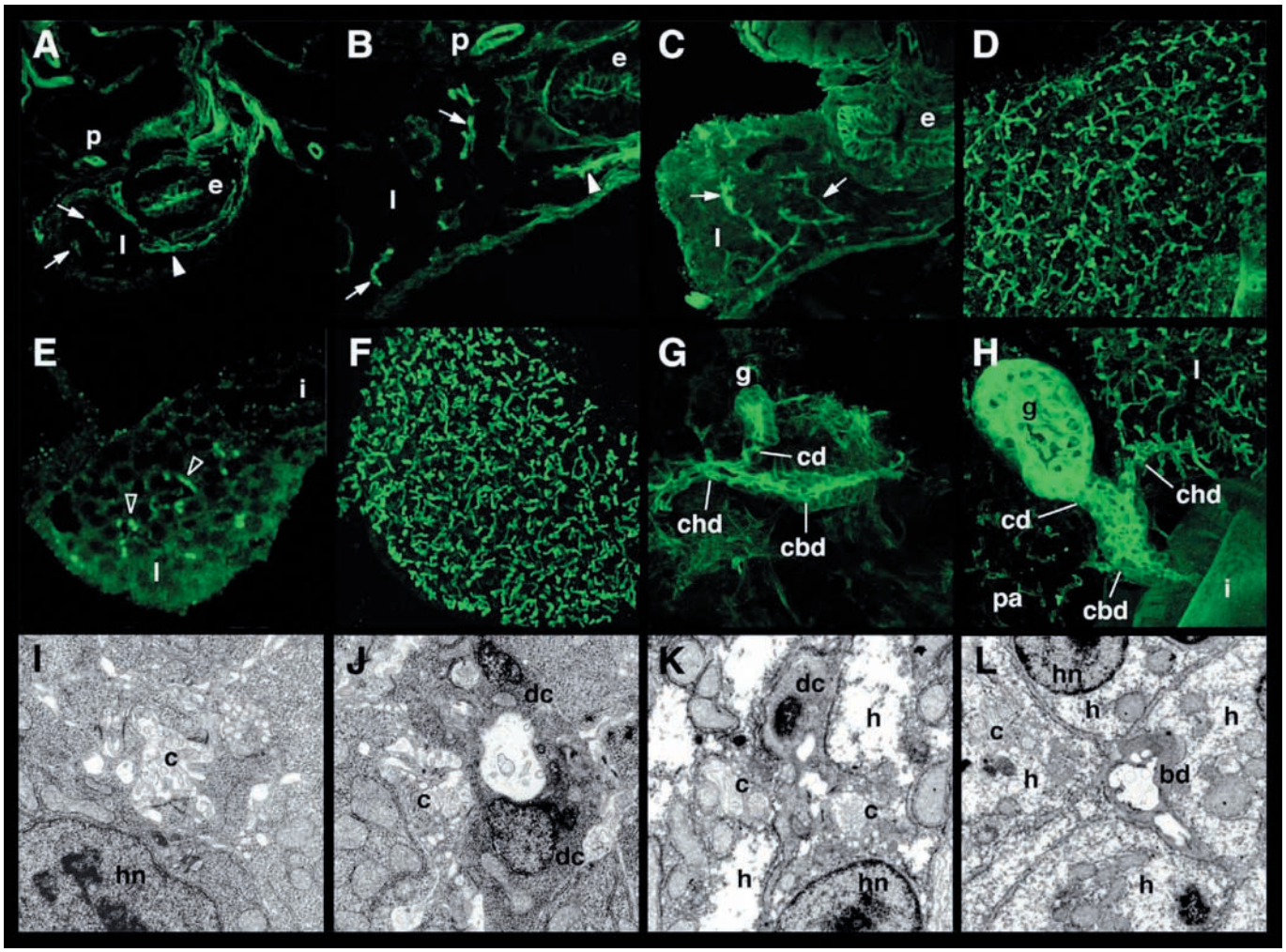

Fig. 3. Zebrafish intrahepatic biliary development. (A-C) Tissue cross-sections of 60-hpf (A) and 70-hpf (B) embryos and a 80-hpf larva (C) processed for cytokeratin IHC. Nascent ducts (arrows) within the developing liver are evident at 60 hpf (A) and 70 hpf (B). By 80 hpf (C), a branching ductular network (arrows) is evident. Arrowheads in A,B indicate the origin of the extrahepatic duct. (D) Confocal projection of intrahepatic bile ducts in a 5-dpf larva processed for cytokeratin IHC. (E) Tissue section of a 70-hpf larva processed for P-glycoprotein IHC. Developing canaliculi (arrowheads) are evident between adjacent hepatocytes. (F) Confocal projection of hepatocyte canaliculi within the liver of a 5-dpf larva – note the elongated, tubular canalicular structure. (G,H) Confocal projection generated from contiguous Z-sections of a 75-hpf larva (G) and a 5-dpf larva (H) processed for cytokeratin IHC. Intrahepatic bile ducts emerge from the liver to form the common hepatic duct (chd), and join the cystic duct (cd) and common bile duct (cbd) that inserts into the intestine (i). (I) Transmission electron micrograph of a 70-hpf larva, showing a developing canaliculus (c) near the hepatocyte nucleus (hn). (J) Canaliculus of a 70-hpf larva anastomosing with a bile duct composed of two ductular cells (dc). (K,L) Transmission electron micrograph from a 5-dpf larva, showing a ductular cell within a hepatocyte tubule anastomosing with several canaliculi from surrounding hepatocytes (K). (L) Distal portion of a bile duct within the center of a hepatocyte tubule. Electron-dense particles within bile are evident in the duct lumen. e, esophagus; g, gall bladder; l, liver; pa, pancreas; p, pronephric duct.

fish is also present in zebrafish (Tanuma, 1980; Yamamoto, 1964).

In mammals, bile is transported from the intrahepatic biliary system to the gallbladder and intestine through large extrahepatic ducts. Mammalian and zebrafish extrahepatic ductular systems are organized in a similar fashion (Fig. 3H). Bile exits the zebrafish liver through a prominent duct we term the common hepatic duct. The common hepatic duct joins the gallbladder via a duct that is comparable to the mammalian cystic duct. Distal to the zebrafish cystic duct, the duct we term the common bile duct carries bile to the intestine. The zebrafish common bile duct joins the intestine in close proximity to the pancreatic duct, as in mammals. This anatomical arrangement persists in juvenile and adult fish (not shown).

Zebrafish biliary development

The zebrafish liver develops from endodermal progenitors that are specified to a hepatic fate at early somite stages (Wallace and Pack, 2003). Although mammalian liver progenitors are specified at a nearly identical developmental stage (Zaret, 2002), gene expression studies and immunohistochemical analyses using liver markers show that the zebrafish liver anlage is first identified at a comparably later stage than the mammalian liver bud (Field et al., 2003; Wallace and Pack,

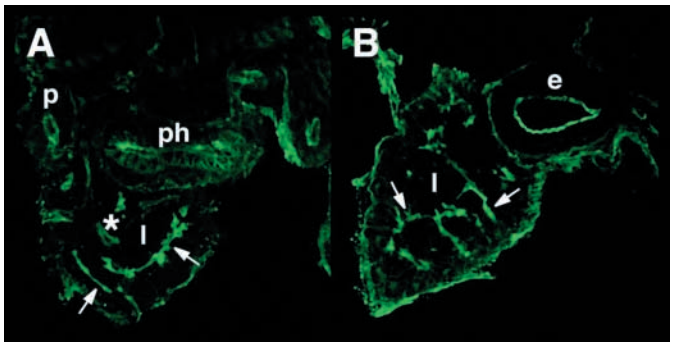

Fig. 4. Zebrafish intrahepatic biliary development occurs independently of liver vasculature. (A,B) Histological cross-sections through the liver of wild-type (A) and *cloche* mutant (B) 80-hpf embryos processed for cytokeratin IHC. Developing bile ducts (arrows) are present in both wild-type and *cloche* embryos. e, esophagus; l, liver; ph, pharynx; p, pronephric duct. Asterisk indicates sinusoids.

2003; Zaret, 2002). To determine what aspects of biliary development are comparable in teleosts and mammals, we determined the timing of bile duct formation using cytokeratin IHC. Biliary cells were first identified in the zebrafish liver between 50 hours post-fertilization (hpf) and 60 hpf (Fig. 3A). Clearly defined, duct-like structures were first evident at 70 hpf (Fig. 3B). By 80 hpf, a branching network of ducts was apparent (Fig. 3C). Confocal projections of whole-mount specimens documented significant growth of the biliary system at subsequent stages (Fig. 3D). TEMs at 70 hpf and 5 days post-fertilization (dpf) confirmed the cytokeratin immunostainings. These showed small bile ducts composed of ductular cells that anastomose with canaliculi of surrounding hepatocytes (Fig. 3J-L). Such findings are compatible with a tubular liver architecture.

Development of the proximal and distal components of the biliary system was also determined. P-glycoprotein IHC and TEMs identified canaliculi within the liver of 70-hpf larvae (Fig. 3E,I). Analyses at subsequent stages revealed elaboration of the tubular canaliculi (Fig. 3F). The cytokeratin marker identified the gallbladder (not shown) and the common hepatic duct at 60 hpf (Fig. 3A), the stage when the smallest intrahepatic biliary radicles were revealed by cytokeratin IHC. Although the precise timepoint when the intrahepatic and extrahepatic systems were first contiguous could not be determined, analyses of histological sections and specimens processed for cytokeratin IHC show this conclusively at 75 hpf (Fig. 3G).

Zebrafish intrahepatic bile ducts develop independently of liver vasculature

Mammalian interlobular bile ducts develop from ductal plate hepatoblasts adjacent to portal vein radicles. Although expression of Jagged ligands and Notch receptors within ductal plate hepatoblasts and adjacent portal regions has been reported (Loomes et al., 2002; Louis et al., 1999; McCright et al., 2002), identification of the cells that supply the Notch signal is uncertain. Portal tract endothelia and its surrounding mesenchyme are considered to be likely candidates (Shiojiri, 1984; Shiojiri and Koike, 1997).

Because our histological studies suggested that zebrafish cholangiocytes do not develop in close proximity to liver vasculature, we were curious about whether endothelial cells played a role in zebrafish biliary development. Analysis of the zebrafish mutant *cloche*, which lacks head and trunk endothelium, as well as most blood cells (Stainier et al., 1995; Liao et al., 1997), allowed us to address this question. As shown in Fig. 4, bile ducts were identified in *cloche* larvae that could be processed for cytokeratin IHC. Importantly, sinusoidal endothelia normally present at this developmental stage could not be identified in these mutants. From this, we conclude that the early stages of biliary development in zebrafish occur independently of vascular endothelia.

Multiple *jagged* ligand and *notch* receptor genes are expressed in the developing zebrafish liver

Identification of Jagged 1 mutations in individuals with AGS established a role for the Notch signal in mammalian biliary development. Notch signaling is known to play a role in various aspects of zebrafish development (Appel et al., 2001; Cornell and Eisen, 2002; Itoh et al., 2003; Lawson et al., 2001). We assayed *notch* receptor and *jagged* ligand expression patterns in the developing liver as a first step in assessing the importance of the Notch signal for zebrafish biliary development.

Multiple zebrafish *jagged* (GenBank Accession numbers AF229448, AF229449 and AF229451) and *notch* genes (Bierkamp and Campos-Ortega, 1993; Itoh et al., 2003; Kortschak et al., 2001) have been identified. *jagged 1*, *2* and *3* are each expressed within the liver at 2 dpf (not shown) and 3 dpf (Fig. 5A-C), the stage when bile ducts form. Expression of *jagged 2* was most pronounced. *notch 1a*, *notch 1b*, *notch 2 and notch 5* (also known as *notch 3*) are also expressed in the liver at these time points (Fig. 5D-G). Histological sections of specimens processed for whole-mount in situ hybridization showed that the *notch 2*, *5* and *jagged 2*, *3* genes were expressed in a uniform pattern within the liver primordium (not

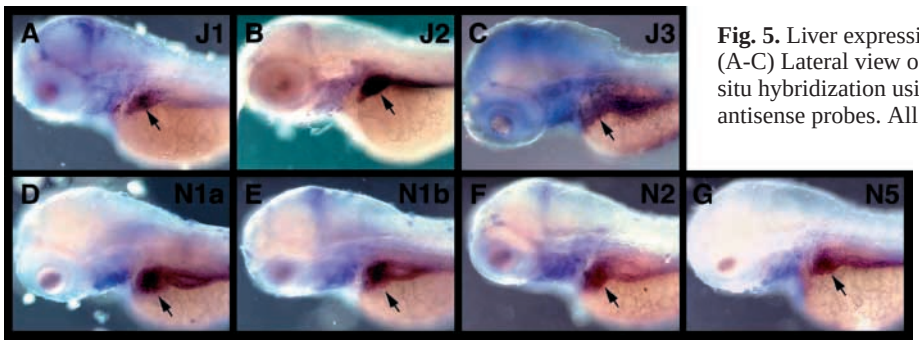

Fig. 5. Liver expression of zebrafish *jagged* and *notch* genes. (A-C) Lateral view of wild-type 72-hpf larvae processed for RNA in situ hybridization using *jagged 1* (A), *jagged 2* (B) and *jagged 3* (C) antisense probes. All three *jagged* genes are expressed in the larval liver (arrow), but *jagged 2* expression is most pronounced. Expression in the branchial arches is also evident. (D-G) Lateral view of wild-type 72-hpf larvae processed for RNA in situ hybridization using *notch 1a* (D), *notch 1b* (E), *notch 2* (F) and *notch 5* (G) probes. All *notch* genes are expressed in the developing larval liver and the branchial arches.

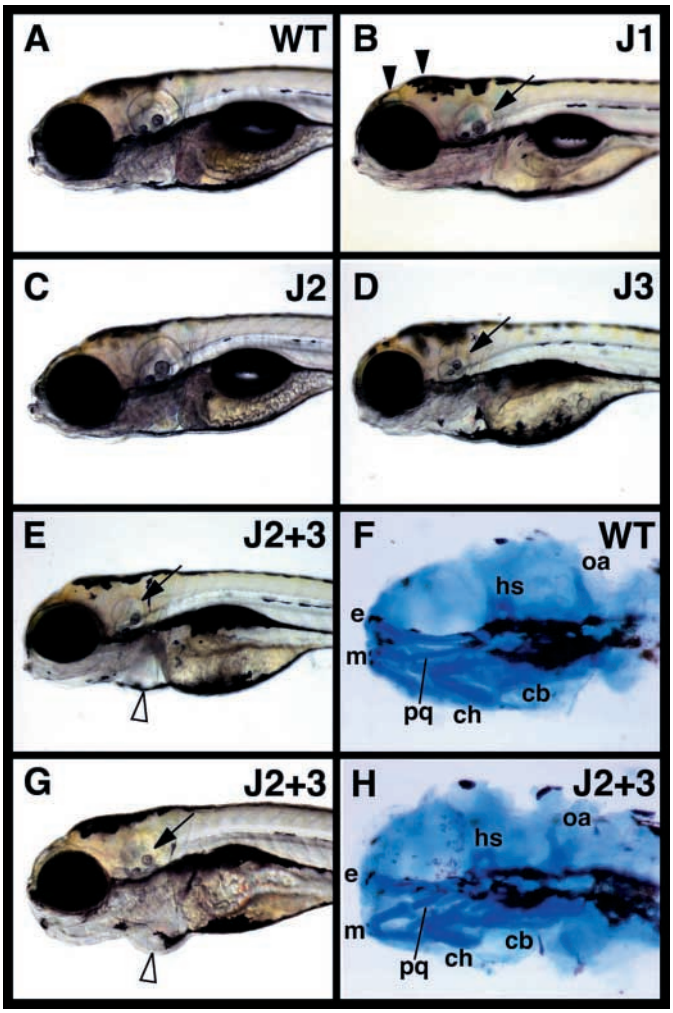

Fig. 6. *jagged* gene knockdowns perturb craniofacial and cardiac development. (A-E,G) Lateral views of (A) wild type, and (B) *jagged 1*, (C) *jagged 2*, (D) *jagged 3* and (E,G) *jagged 2/3* morphants. Note, forebrain and midbrain defects in *jagged 1* morphants (arrowheads) and mild craniofacial defects in the *jagged 3* (D) and *jagged 2/3* (E,G) morphants. All morphants, except *jagged 2*, have small ears (arrows). *jagged 2/3* morphants have pericardial edema (open arrowhead). (F,H) Alcian Blue staining of 5-dpf wild-type (F) and *jagged 2/3* morphant (H) larvae, lateral view. These stainings show that the ethmoid (e), palatoquadrate (pq) and ceratohyal (ch) cartilages of *jagged 2/3* morphants are smaller than in wild-type siblings. Similar findings are observed in *jagged 3* morphants (not shown). cb, ceratobranchial; hs, hyosymplectic; m, Meckel's cartilage; oa, occipital arch.

shown). These expression patterns suggested that these *notch* orthologs might play a role in zebrafish biliary development.

Jagged-mediated Notch signaling regulates zebrafish intrahepatic bile duct development

Gene knockdowns were performed to assess the role of Jagged-mediated Notch signaling in zebrafish biliary development. For these analyses, morpholinos were injected into 1- to 4-cell stage fertilized embryos, which were then assayed at 5 dpf for bile duct development using cytokeratin IHC. Developing morphants were inspected daily for defects in cardiac and craniofacial development. Morpholinos to the 5′ region of *jagged 1*, *2* and *3* were injected both alone and in combination with each other. Specificity of the morpholinos was confirmed using an in vitro translation assay (data not shown).

We initially assayed the effects of *jagged* gene knockdowns because the majority of individuals with AGS are haploinsufficient for human Jagged 1 (Piccoli and Spinner, 2001). We observed that high dose *jagged 1* morphants had severe developmental delays and extensive cell death, and that low dose *jagged 1* morphants had subtle forebrain and midbrain defects, and small ears (Fig. 6B). *jagged 2* morphants appeared normal or occasionally had cardiac edema (Fig. 6C). *jagged 3* morphants had mild craniofacial abnormalities, smaller ears and, infrequently, cardiac edema (Fig. 6D). Nearly all *jagged 2/3* morphants had craniofacial defects and pericardial edema (Fig. 6E,G,H). Liver size was normal in nearly all morphants, as was extrahepatic bile duct and gallbladder development (Fig. 7I).

Cytokeratin IHC was used to analyze biliary development in the various *jagged* morphants. The intrahepatic biliary system of *jagged 1*, *jagged 3* (Fig. 7B,E), and compound *jagged 1/2* (Fig. 7F) and *jagged 1/3* (not shown) morphants developed normally. Intrahepatic biliary development was perturbed in a dose-dependent manner in *jagged 2* morphants. The majority of bile ducts in embryos injected with low doses of the *jagged 2* morpholino developed normally (Fig. 7C). Occasional rosettes of liver cells with apical cytokeratin were identified in all of these larvae. With high doses of the *jagged 2* morpholino, rosettes were more frequent, and the density of ducts was diminished (Fig. 7D). Co-injection of a *jagged 3* morpholino (Fig. 7F), but not a *jagged 1* morpholino (Fig. 7G), augmented the biliary defect of both the low dose and high dose *jagged 2* knockdowns. In the *jagged 2/3* morphants, few if any recognizable bile ducts were observed, and rosettes were prominent. By contrast, extra-hepatic biliary development was normal in these larvae (Fig. 7I). Importantly, co-injection of a full-length human *Jagged 1* mRNA, but not a truncated *Jagged 1* mRNA, rescued the biliary phenotype in 20% of morphant larvae analyzed (Fig. 7H). By contrast, co-injection of an mRNA for *hnf6*, a gene which regulates mammalian (Clottman *et al*., 2002) and zebrafish biliary development (Matthews et al., 2004), and that is expressed at reduced levels following *jagged 2/3* knockdown (see Fig. S1 in supplementary material), did not rescue the morphants.

Histological sections of the *jagged 2/3* morphants processed for cytokeratin (Fig. 8D,E) and P-glycoprotein (Fig. 8F,I) IHC, and also ultrastructural analyses (Fig. 8G,H), showed that the cytokeratin (cholangiocyte) marker co-localized with microvilli and immunoreactive P-glycoprotein characteristic of the hepatocyte canaliculus. Consistent with a defect of biliary development, ductular cells were never seen within these hepatocyte rosettes. Co-localization of the cytokeratin and canalicular markers within *jagged 2/3* morphant liver cells suggests these cells may be cholangiocyte-hepatocyte hybrids. Reduced P-glycoprotein staining in the morphant liver suggests that the hepatocyte differentiation program has been altered in many hybrid cells. Together, these findings suggest that Notch signaling regulates a binary cell fate decision in the developing zebrafish liver. Consistent with this early role for Notch signaling in cholangiocyte development, hepatocyte rosettes are already observed in *jagged 2/3* morphant embryos at early

stages of bile duct formation (74 hpf; not shown), whereas they are never seen in sibling wild-type larvae at this stage.

Compound *jagged* gene knockdowns produce multi-organ defects suggestive of a zebrafish Alagille Syndrome phenocopy

The presence of biliary defects but normal gallbladder and extrahepatic bile duct development in *jagged* morphants is suggestive of an AGS phenocopy. To confirm this, we sought to determine whether other AGS target organs were affected by the *jagged* knockdowns.

Craniofacial alterations are common in individuals with AGS. One aspect of the characteristic faces of AGS children (triangular face) involves the alteration of facial bones that in part derive from the first and second pharyngeal arch (maxilla and mandible). *jagged 1* is also strongly expressed at a similar location during mouse development (Kamath et al., 2002a). We observed that knockdown of zebrafish *jagged* genes altered the size of facial cartilages that are derived from the first and second branchial arches (palatoquadrate, Meckel's and ceratohyal cartilages; Fig. 6F,H). Although a detailed description of craniofacial defects in individuals with AGS has not been reported, we considered the zebrafish craniofacial defects associated with *jagged* knockdowns to be compatible with a partial AGS phenocopy.

The pancreas is also affected in individuals with AGS. Pancreatic insufficiency is considered a clinical manifestation of AGS (Chong et al., 1989; Krantz et al., 1997; Emerick et al., 1999). We observed that pancreatic ductular development was altered in *jagged 2/3* morphants and considered these changes compatible with an AGS phenocopy, because they would severely impair exocrine function. *jagged 2/3* morphants had few intra-pancreatic ducts (Fig. 9B,F,I), whereas the extra-pancreatic duct that joins the pancreas to the intestine developed normally. By contrast, morphant acini were enlarged but composed of cells that had normal carboxypeptidase A levels (Fig. 9D,H) and a normal ultrastrucure (not shown). Interestingly, apical cytokeratin was also identified in the acinar cells of the morphant larvae (Fig. 9F,I). Although the precise etiology of pancreatic insufficiency in individuals with AGS is not known, ductal defects, such as those we observe and that also occur in other heritable diseases, such as cystic fibrosis, could explain this finding.

Kidney development, which is altered in individuals with AGS, was also affected in *jagged 2/3* morphants. Compared with wild-type siblings, glomeruli in 5-dpf morphants were small and in these larvae, vascular elements were difficult to recognize (see Fig. S2A,B in supplementary material). In other larvae, segments of the glomerulus were replaced by dilated blood vessels resembling aneurysms (Fig. S2A,C). These findings closely resemble the kidney defects reported to occur in mouse models of AGS (McCright et al., 2001).

Tubular defects were also seen in all *jagged 2/3* morphants. Proximal kidney tubules of all morphants were filled with amorphous debris that is normally present in early stage wild-type embryos (see Fig. S2D-F in supplementary material). Many tubules had an irregular contour and were lined by dysmorphic epithelia. These findings are important because

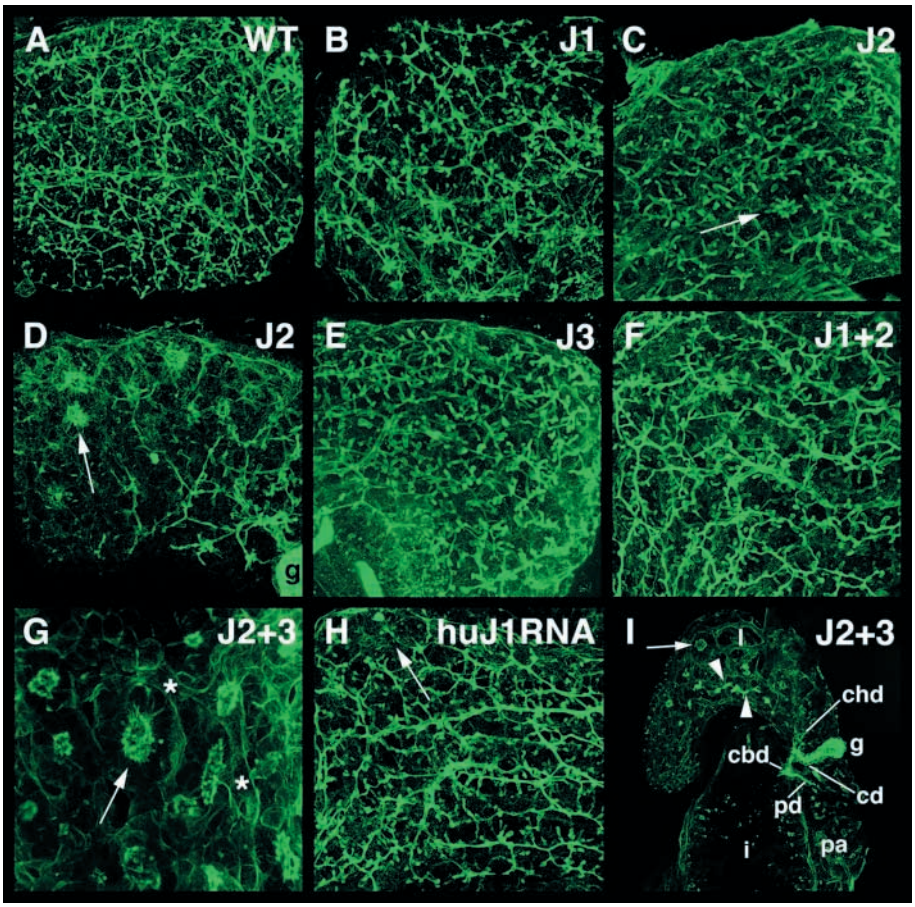

Fig. 7. *jagged 2* and *jagged 3* regulate development of the zebrafish intrahepatic biliary system. (A-I) Confocal projections through the liver of 5-dpf zebrafish larvae processed for cytokeratin IHC. Intrahepatic biliary development is normal in *jagged 1* (B), *jagged 3* (E), *jagged 1/2* (F) and *jagged 1/3* (not shown) morphants, when compared to wild type (A). Biliary development is abnormal in *jagged 2* morphants. In low-dose *jagged 2* morphants (C), rosettes of liver cells with apical cytokeratin staining are noted (arrow). High-dose *jagged 2* morphants (D) have frequent rosettes (arrow) and a small complement of normal bile ducts. Co-injection of the *jagged 3* morpholino with either a low dose (G), or high doses (not shown), of the *jagged 2* morpholino severely disrupts intrahepatic bile duct development. These larvae have few recognizable bile ducts. Instead, immunoreactive cytokeratin is located apically, within hepatocyte rosettes (arrow), or along vascular sinusoids (asterisk) that in teleosts normally express low levels of cytokeratins. (H) Twenty percent of larvae co-injected with full-length human *Jagged 1* mRNA and *jagged 2/3* morpholinos have only rare rosettes (arrow). (I) Low-power confocal projection showing normal gallbladder and extrahepatic bile duct development in a *jagged 2/3* morphant larva. Arrow indicates liver cell rosette; arrowhead indicates origin of common hepatic duct (chd) within the liver. cbd, common bile duct; cd, cystic duct; chd, common hepatic duct; g, gallbladder; i, intestine; l, liver; pa, pancreas; pd, pancreatic duct.

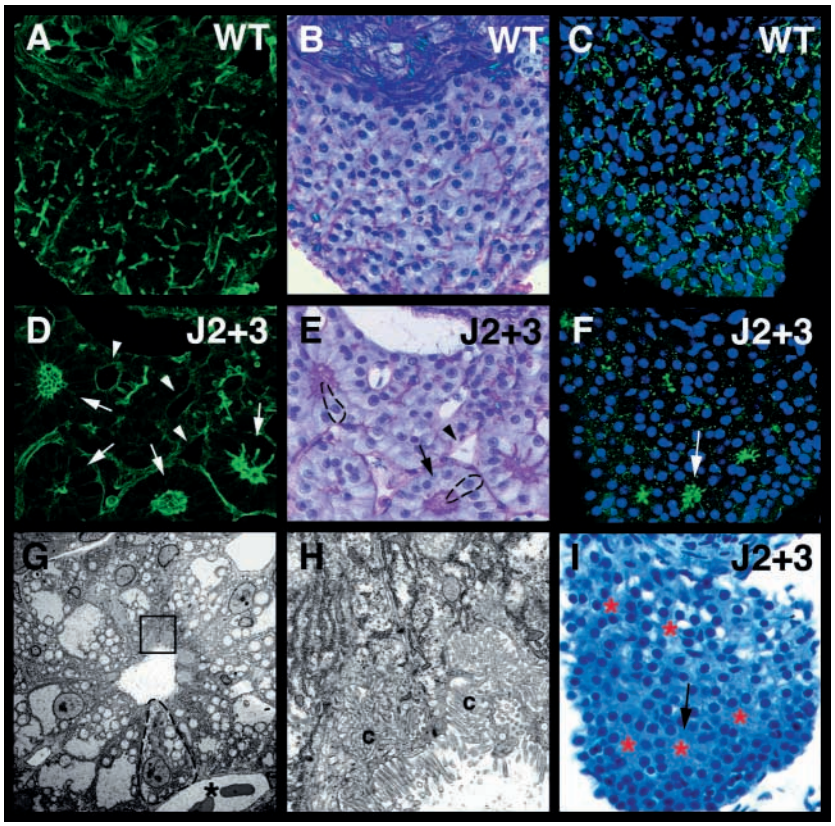

Fig. 8. Jagged-mediated Notch signaling may regulate a binary cell-fate decision of zebrafish hepatoblasts. (A-F,I) Histological sections through the liver of 5-dpf wild-type (A-C) and *jagged 2/3* morphant (D-F,I) larvae processed for cytokeratin and P-glycoprotein IHC. (A) A Branching network of bile ducts is evident in this wild-type larva. (B) Section in A processed for histology with superimposed pseudocolored cytokeratin pattern (magenta). (D) Four hepatocyte rosettes (arrows) are shown in this section through the liver of a *jagged 2/3* morphant larva. Weak cytokeratin expression is also present in endothelial cells lining sinusoids seen in cross-section (arrowheads). (E) Section in D processed for histology with superimposed pseudocolored cytokeratin pattern (magenta). These sections show cytokeratin within the apical region of rosette cells (arrow indicates one of the four rosettes identified in D) and in surrounding sinusoidal endothelial cells (arrowhead). Dashed lines outline individual hybrid cells in two hepatocyte rosettes. (C,F) Wild-type (C) and *jagged 2/3* morphant (F) larvae processed for P-glycoprotein IHC. Individual canaliculi are seen in the liver of wild-type larvae. In morphants, the P-glycoprotein is clustered in the central region of rosettes (arrow points to middle rosette). Compared with wild type, there is much less P-glycoprotein staining in the morphant liver. (I) Section shown in F stained for histological analysis. Red asterisks identify the location of P-glycoprotein+ cells (F). (G,H) Electron micrographs through the liver of 5-dpf *jagged 2/3* morphant larvae. Low-power view (G) shows rosette cells with apical canaliculi (c), best appreciated in a high power view (H). Ultrastructurally, cells comprising the rosettes (dashed line in G) resemble hepatocytes. However, cytokeratin, a biliary marker, is also located apically in these cells (D).

renal tubular acidosis, which arises from kidney tubule defects, occurs in individuals with AGS (Emerick et al., 1999).

Finally, nearly all *jagged 2/3* morphant larvae developed cardiac edema that was rescued by co-injection of human *Jagged 1* mRNA (see Table S1 in supplementary material). Although cardiac edema in zebrafish larvae may be a non-specific finding, several lines of evidence suggest it may arise from a mild outflow tract defect in *jagged 2/3* morphants. First, histological analysis did not reveal gross architectural defects of the endocardium, myocardium or cardiac valves of morphant larvae (not shown). Second, cardiac chamber size and orientation were also normal in the morphants. Third, the presence of cardiac edema did not correlate with the glomerular defects that may also be expected to cause edema; for example, we observed pronounced glomerular abnormalities in non-edematous larvae. Given that mild outflow tract defects are the most common cardiac abnormalities in individuals with AGS, and that these defects rarely cause severe cardiac dysfunction, we believe that cardiac edema in *jagged* morphants is compatible with an AGS phenocopy.

Multiple *notch* family members play a role in zebrafish intrahepatic biliary development

Although AGS can arise in the setting of haploinsufficiency for Jagged 1, mice engineered to carry one copy of *jagged 1* develop in a nearly normal fashion (Xue et al., 1999). However, biliary, cardiac and other defects suggestive of AGS develop in mice homozygous for a hypomorphic allele of *notch 2* (McCright et al., 2001; McCright et al., 2002), and in mice heterozygous for this *notch 2* allele and a null allele of *jagged 1* (McCright et al., 2002). For these reasons, we analyzed the effect of zebrafish *notch* receptor gene knockdowns both alone, and in combination with various *jagged* ligands.

The *notch 2/5* morphants were analyzed first because both genes are prominently expressed in the developing liver. Knockdowns of *notch 2* alone did not affect biliary development (Fig. 10B). Knockdowns of *notch 5* had a mild effect; hepatocyte rosettes were observed in a small number of *notch 5* morphants (Fig. 10C). By contrast, combined *notch 2/5* knockdowns had a prominent effect on biliary development. Hepatocyte rosettes were present in all morphant larvae (Fig. 10D). However, the severity of the biliary phenotype was less pronounced than that seen with combined *jagged 2/3* knockdowns. Bile ducts were seen infrequently in *jagged 2/3* morphants but were identifiable in all *notch 2/5* morphants. These findings suggested that a third zebrafish Notch receptor might play a role in biliary development. For this reason, we also analyzed larvae that had been injected with morpholinos to *notch 1a* and *notch 1b* alone, and in combination with each other and the *notch 2* and *notch 5* morpholinos. In these experiments biliary development was either normal, or not interpretable because of severe developmental delays (not shown). Thus, a role for a third Notch receptor in zebrafish biliary development could not be confirmed.

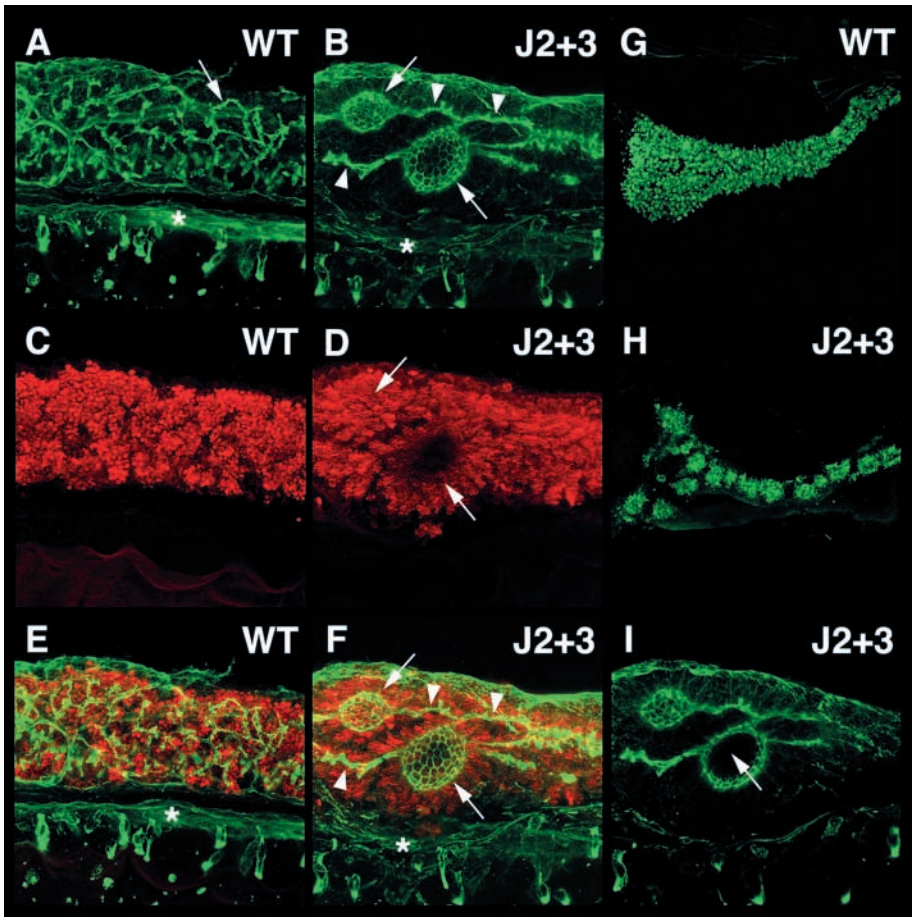

Fig. 9. Jagged-mediated Notch signaling regulates pancreatic duct development. Confocal projections through the posterior pancreas of 5-dpf wild-type (A,C,E) and *jagged 2/3* morphant (B,D,F,I) larvae processed for cytokeratin IHC (green; duct marker), and carboxypeptidase (red; acinar cell marker) IHC. (A) Immunoreactive cytokeratin outlines ducts within the wild-type pancreas (arrow), as well as a large ventral blood vessel (*). (B) Only a few large ducts (arrowheads) are visible in *jagged 2/3* morphants. Most regions of the morphant pancreas are devoid of ducts and instead contain enlarged acini (arrows) that ectopically express cytokeratin. Acinar structure in morphant larvae was confirmed ultrastructurally (not shown). (C) Immunoreactive carboxypeptidase A (red) is localized in small acini in the wild-type pancreas. (D) Acini in 5-dpf *jagged 2/3* morphants are enlarged (arrows) and may have dilated lumens (lower arrow). Acinar cells express carboxypeptidase A (red). (E,F) Superimposed confocal projections through wild-type and *jagged 2/3* morphant pancreas shown in A and C, and B and D, respectively. The acinar cells within the enlarged morphant acini (arrows in F) ectopically express the cytokeratin duct marker on the apical and lateral cell surface of the acinar cells. (I) Thin optical section (10 μm) through the lumen of the larger acinus depicted in B and F, showing apical cytokeratin in cells lining the acinar lumen (arrow). (G,H) Low power, whole-mount image of the 5-dpf wild-type (G) and *jagged 2/3* morphant (H) larval pancreas; larvae processed for carboxypeptidase A IHC (green). Note the enlarged, dispersed acini in the *jagged 2/3* larvae (H) compared with wild-type sibling (G).

Studies in the mouse have shown that mutant alleles of *jagged 1* and *notch 2* fail to complement one another in compound heterozygous animals and instead produce an AGS phenocopy (McCright et al., 2002). Gene dosage has been postulated as one possible mechanism to explain this finding. Analyses of zebrafish compound *jagged*/*notch* morphants support this model. Compound *jagged 2*/*notch 2*, and *jagged 2*/*notch 5*, morphants had severe biliary defects that were identical to the *jagged 2/3* morphants (Fig. 10E,F). By contrast, biliary development was either normal or only mildly affected in *jagged 1*/*notch 2*, *jagged 1*/*notch 5*, *jagged 3*/*notch 2* and *jagged 3*/*notch 5* morphants (Fig. 10G and not shown).

Taken together, these data support a primary role for the *notch 2* and *notch 5* receptors in zebrafish biliary development. Our experiments could not exclude the possibility that signaling through another Notch family member may also play a minor role in biliary development. Alternatively, less severe biliary defects associated with compound Notch knockdowns may be explained by a reduced efficacy of the *notch 2* and *notch 5* morpholinos when compared with the *jagged* morpholinos. The finding that the *jagged 3*/*notch 2* knockdown had no effect on biliary development compared with the *jagged 2*/*notch 2* knockdown is consistent with the identification of *jagged 2* as the principal Notch ligand directing biliary development.

Ectopic activation of the Notch signal promotes biliary development

The appearance of cells with the characteristics of hepatocytes and biliary cells in the setting of reduced Notch activity suggests the Notch signal normally regulates differentiation of a biliary progenitor cell. Alternatively, Notch may be responsible for the maintenance of a more differentiated progenitor in whose absence hepatocyte/biliary hybrid cells emerge. With the former model, the activation of Notch signaling is predicted to increase the number of biliary cells.

To test this hypothesis, we analyzed biliary development in larvae expressing a heat shock-inducible *hsp70:Gal4* transgene in combination with a *UAS:notch1aICD* allele (Scheer et al., 2002). Following heat shock, transcription of the Gal4-responsive, constitutively active *notch1aICD* allele ensues. For these experiments, Notch signaling was activated in transgenic fish and non-transgenic clutch mates via heat shock (40°C×30 minutes) at 12 hour intervals beginning at 48 hpf. Heat-shocked larvae were processed for cytokeratin IHC 12 hours after the final heat shock.

Following this protocol, we analyzed 72-hpf larvae that had been heat-shocked at 48 hpf and 60 hpf, 84-hpf larvae heat-shocked at 60 hpf and 72 hpf, and 96-hpf larvae heat-shocked at 72 hpf and 84 hpf. Cytokeratin IHC showed enlarged, ectopic biliary ducts in all heat-shocked larvae carrying the

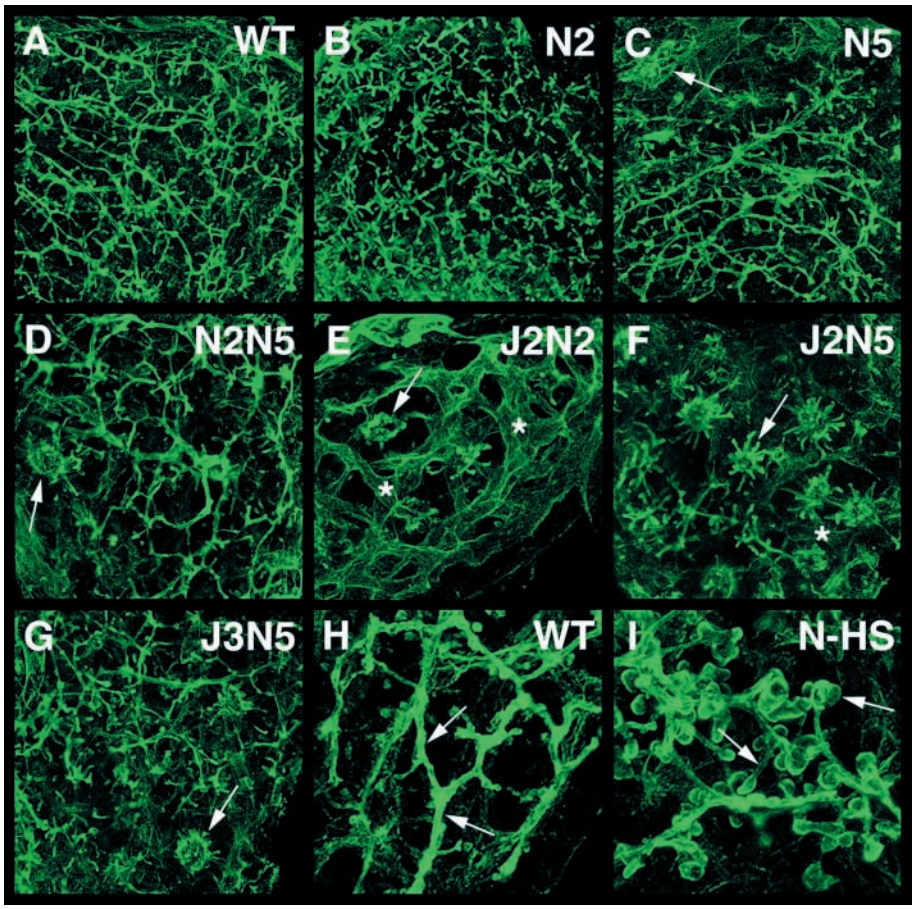

Fig. 10. Multiple Notch receptors regulate zebrafish intrahepatic biliary development. (A-I) Confocal projections through the liver of 5-dpf zebrafish larvae processed for cytokeratin IHC. (A) Wild-type intrahepatic biliary ducts. (B) Normal biliary development in *notch 2* morphants. (C) Rare hepatocyte rosettes are seen in *notch 5* morphants (arrow). (D) *notch 2*/*5* morphants have rosettes (arrow) and reduced duct density. (E,F) Severe biliary defects in *jagged 2*/*notch 2* and *jagged 2*/*notch 5* morphants. Note rosettes (arrows) and also pronounced vascular cytokeratin staining in the *jagged 2*/*notch 2* morphant. (G) *jagged 3* knockdown does not augment the mild *notch 5* morphant biliary phenotype (arrow, rosette). (H,I) 96-hpf *hsp70:GAL4* and *hsp70:GAL4; UAS:notch1aICD* transgenic larvae processed for cytokeratin IHC. Ectopic biliary ducts (arrows) are only visible in the bigenic larvae following heat shock at 74 hpf and 86 hpf. Asterisk indicates endothelial cytokeratin staining.

notch1aICD and *GAL4* transgenes. These ectopic ducts were best appreciated in 96-hpf larvae (Fig. 10H,I), but were also identifiable at earlier timepoints (see Fig. S3 in supplementary material). Immunostaining of heat-shocked larvae with the P-glycoprotein antibody showed that the canaliculi were also enlarged (see Fig. S4 in supplementary material). Histological analyses of heat-shocked transgenic larvae allowed us to quantitate the effects of Notch activation (not shown). This showed a 40% increase in the number of small biliary ducts in 96-hpf heat-shocked transgenic larvae, when compared with heat-shocked fish lacking the *UAS:notch1aICD* transgene (n=49 transgenic ducts per field, range 44-55; versus n=35 wild-type ducts per field, range 28-41).

The reciprocal effects of Notch inhibition and activation on biliary development, coupled with the presence of hybrid cells in *jagged* and *jagged*/*notch* morphant larvae, are supportive of a model in which the Notch signal promotes the development of biliary cells from a bipotential progenitor.

Discussion

Alagille syndrome is a heritable disorder that affects multiple organ systems. Dominant mutations in Jagged 1 are identified in greater than 70% of individuals with AGS and it is predicted that the majority of people diagnosed with AGS will ultimately be shown to have Jagged 1 defects (Piccoli and Spinner, 2001). Cholestatic liver disease is present in nearly all individuals with AGS, as originally defined, and in the past has been considered to be an essential criterion for the AGS diagnosis. However, reports that first-degree relatives of AGS patients can have cardiac and other organ defects typical of AGS in the absence of overt liver disease, and a recent report of a series of Jagged 1 mutations in individuals with isolated congenital cardiac defects, suggest that the spectrum of defects caused by Jagged 1 mutations is broad (Elmslie et al., 1995; Emerick et al., 1999; Kamath et al., 2002b; McElhinney et al., 2002).

Current models of AGS suggest that haploinsufficiency for Jagged 1 is responsible for AGS, although a dominant-negative mode of inheritance for some Jagged 1 mutations has not been fully excluded (Piccoli and Spinner, 2001). Studies in the mouse support a haploinsufficiency model. Homozygous *jagged 1* mutant mice die from widespread hemorrhage at early stages (Xue et al., 1999). However, heterozygous *jagged 1* mutant mice develop mild ocular defects suggestive of AGS, and compound mutant mice that are heterozygous for a deletion allele of *jagged 1* and a hypomorphic allele of *notch 2* develop cardiac and biliary defects typical of AGS (McCright et al., 2002). Furthermore, mice homozygous for a hypomorphic *notch 2* allele lack intrahepatic bile ducts and have cardiac and kidney defects consistent with an AGS phenocopy (McCright et al., 2001; McCright et al., 2002), whereas mice homozygous for a null allele of *notch 2* die at early stages (Hamada et al., 1999). Together, these data suggest a conserved role for Notch signaling in mammalian biliary, heart, kidney and ocular development that is sensitive to gene dosage (McCright et al., 2002).

Perturbation of Jagged-mediated Notch signaling in zebrafish identifies an evolutionarily conserved pathway that directs bile duct development

Knockdowns of zebrafish *jagged* genes, alone or in combination with *notch* genes, perturb zebrafish biliary, pancreatic, cardiac, kidney and craniofacial development. We

believe such defects are compatible with an AGS phenocopy. In this report, we have focused principally on the role of Notch signaling in zebrafish bile duct formation. Bile duct paucity on liver biopsy is a nearly universal feature of Alagille patients with liver disease. It is present in some individuals with AGS at birth, but develops in the majority of cases within 6 months (Piccoli and Witzleben, 2001). Thus, many individuals with AGS are born with a significant number of intrahepatic bile ducts that are either lost or do not expand during the first months of postnatal life, as a result of reduced Notch signaling. Whether Notch-mediated biliary expansion involved proliferation of existing ducts or the recruitment of new biliary cells (cholangiocytes) is not known.

Phenocopy of AGS in zebrafish using morpholino-mediated knockdown may be predicted to be difficult because precise titration of the *jagged* gene levels is not feasible. However, we observed that *jagged 2* morphants have mild to moderate intrahepatic biliary defects, but that compound *jagged 2*/*3* knockdown profoundly disrupted biliary development. Importantly, these defects occur in the setting of continued liver growth and differentiation. Liver size is near normal and sinusoidal vascularization is evident in the most severely affected *jagged 2* and *jagged 2*/*3* morphants. Together, these data confirm a role for Jagged-mediated Notch signaling in zebrafish biliary development.

Although our data do not allow us to speculate on whether Notch signaling promotes biliary development through lateral inhibition, induction or some other mechanism, the presence of ectopic biliary ducts in transgenic larvae engineered to express a constitutively active *notch1a* allele suggests that spatial restriction of some component of the Notch signaling system is important to this process. The presence of ectopic ducts that branch prematurely in Notch-activated larvae supports the idea that the Notch signal promotes biliary development. Whether this effect of Notch activation occurs through the recruitment of new biliary cells or through the growth of existing ducts could not be addressed in this study.

The finding of ectopic ducts in Notch-activated transgenic larvae is important because it does not support a suppressive role for Notch during biliary development. Such a role has been proposed for Notch signaling during mammalian pancreas development (Norgaard et al., 2003). In this model, the Notch signal normally regulates the proliferation and maintenance of undifferentiated pancreatic progenitor cells. Enhanced and premature ductal branching following Notch activation is, in our opinion, more consistent with a model in which Notch directly promotes biliary development rather than maintaining undifferentiated liver progenitors.

Perturbation of Notch signaling in zebrafish causes multi-organ defects compatible with an AGS phenocopy

In addition to the aforementioned biliary defects, we identified other phenotypic features of *jagged* and *jagged*/*notch* morphants that we believe are compatible with an AGS phenocopy (see Table S2 in supplementary material). First, the *jagged 2*/*3*, *notch 2*/*5* and compound *jagged 2*/*notch* morphants had intra-pancreatic ductal defects. Such defects would be predicted to lead to exocrine pancreatic insufficiency, which is recognized as a clinical manifestation of AGS. Although the pathophysiology of exocrine insufficiency in AGS is not well characterized, our data point to a role for a ductal defect. Reports of pancreatic cysts and fibrosis in individuals with AGS are also compatible with this hypothesis (D. Piccoli, personal communication). Further, given that only a small amount of functional exocrine tissue is required to avert symptomatic exocrine insufficiency (Pandol, 1998), it is not surprising that this is not a more common presenting feature of AGS.

Interestingly, exocrine pancreas and biliary defects associated with perturbation of Jagged-mediated Notch signaling were remarkably similar. This may be expected given that the teleost liver and exocrine pancreas share a similar acinar architecture. Particularly intriguing was the observation that immunoreactive cytokeratin, a ductular marker, accumulated in the apical pole of morphant pancreatic acinar cells. This suggests that Jagged-mediated Notch signaling may also regulate a binary cell fate decision during parenchymal ductular development in both the liver and the pancreas. Whether Delta-mediated Notch signaling, which disrupts mammalian pancreas development at an early stage (Apelqvist et al., 1999), plays a comparable role in early pancreas development in zebrafish was not addressed by our studies.

Kidney defects are common in individuals with AGS. In one series of AGS patients, small kidney size was the most commonly reported structural defect, whereas renal tubular acidosis, which arises from a defect of tubular cells, was the most common functional defect (Emerick et al., 1999). Glomerular abnormalities in AGS patients with renal failure were also reported. The kidney defects we identified in *jagged 2*/*3* morphant larvae resemble these defects and the kidney defects reported in mouse models of AGS (McCright et al., 2001).

Craniofacial defects were another feature of the *jagged* and *jagged*/*notch* morphants that we feel is compatible with an AGS phenocopy. The reduced size of cartilage derived from the first pharyngeal arch is reminiscent of the alterations of the appearance of the mandible and maxillary bones typical of young AGS patients. Presumptive cardiac defects were also seen in the morphants. Although we have not determined a precise etiology for these defects, its relatively late onset, coupled with the absence of overt myocardial or valvular defects in morphant larvae, suggests that outflow tract defects may be likely culprits. Such defects are commonly seen in individuals with AGS (McElhinney et al., 2002). Interestingly, we did not see valvular defects comparable to those reported to occur in zebrafish embryos treated with a pharmacological inhibitor of Notch receptor processing (Timmerman et al., 2004). Taken with our data, this raises the possibility that cardiac valve development in zebrafish is not driven by Jagged-mediated Notch signaling. Alternatively, disruption of cardiac valve formation in zebrafish may require a greater reduction in the dosage of the Notch signal than in other organs. This contrasts with a recent report describing one Jagged 1 mutation that suggests that the developing human heart may be more sensitive to the dosage of Notch signaling than the developing liver (Lu et al., 2003).

One limitation to this study was our inability to quantitate the effectiveness of the various knockdowns. These limitations notwithstanding, we are confident of the specificity of the *jagged* and *notch* knockdowns for several reasons. All morpholinos performed as predicted in in vitro translation

assays. Additionally, internal controls were present for all experiments. For example, only the *jagged 2* and *notch 5* morpholinos perturbed bile duct development when injected on their own. Thus, this effect cannot be considered a non-specific effect of the morpholino injections. Activity of the *jagged 1* and *jagged 3*, and various *notch* morpholinos, that when injected alone had no effect on bile duct development was confirmed by their effects on other organs, or by their modifying effect on *jagged 2*.

Redundancy of *jagged* and *notch* gene function during zebrafish biliary development

Direct phenotypic comparisons of zebrafish *jagged*, *notch* or *jagged*/*notch* morphants with mouse mutants or individuals with AGS is complicated by the existence of a third *jagged* gene within the teleost genome. This is likely to have arisen from a genome-wide duplication that occurred after divergence of the teleost and mammalian vertebrate lineages (Taylor et al., 2003). Partial redundancy of duplicated zebrafish *jagged* gene function is compatible with overlapping *jagged* gene expression patterns at early developmental time points and may explain several aspects of the zebrafish *jagged* morphant phenotypes. Such models of organ-specific gene compensation are compatible with the function of other zebrafish gene families (Dorsky et al., 2003; Henry et al., 2002; Lekven et al., 2003).

Sequence comparisons and conserved gene synteny predict that zebrafish *jagged 3* is the teleost ortholog of mammalian *Jagged 1* (see Fig. S4 in supplementary material). However, functional analyses point to zebrafish *jagged 2* as the principal regulator of intrahepatic biliary development, whereas *jagged 3* plays a predominant role in craniofacial and ear development. The limited predictive value of protein sequence for identifying zebrafish orthologs of closely related mammalian *Gata* genes has been noted previously (Wallace et al., 2003). Within the zebrafish *jagged* gene family, functional differences may be predicted to arise from differences in the timing, location or levels of gene expression within the developing liver. Our RNA in situ studies appear to support the latter possibility. *jagged 2* expression is most pronounced in the liver, whereas *jagged 3* expression is higher in the branchial arches and the ear. Surprisingly, our studies did not identify a role for *jagged 1* in biliary development, despite its prominent liver expression. Whether *jagged 1* plays another, as yet unrecognized role in liver development cannot be excluded.

Multiple *notch* genes are also expressed within the embryonic zebrafish liver and our data suggest that their functions also overlap during biliary development. We examined the role of *notch 2* first because of its defined role in mouse biliary development. We observed that perturbation of zebrafish *notch 2* had little effect on biliary development, whereas knockdown of *notch 5*, which shares greater sequence similarity with mammalian *notch 3* than with zebrafish *notch 2*, produced mild biliary defects. These findings suggested that *notch 5* may play a principal role during biliary development. Alternatively, these findings may arise from a reduced efficacy of the *notch 2* morpholino, which is directed against an exon-intron splice junction, when compared with the *notch 5* morpholino, which is directed against the 5′ region of the *notch 5* gene.

Conserved aspects of vertebrate biliary development

Defects of biliary, pancreas, cardiac and craniofacial development in zebrafish *jagged* and *jagged*/*notch* morphants point to an evolutionarily conserved role for Notch signaling during vertebrate organogenesis. Data from this study identify several other shared features of teleost and mammalian biliary development.

First, the redundancy of *jagged* and *notch* gene function during zebrafish biliary development is compatible with data that point to the importance of the dosage of the Notch signal for biliary development. In humans, AGS arises in the setting of Jagged 1 haploinsufficiency. Similarly, we found that zebrafish biliary development was sensitive to the degree of *jagged 2* knockdown. Surprisingly, haploinsufficiency for *jagged 1* does not produce an AGS phenocopy in mice. However, mice heterozygous for mutant alleles of *jagged 1* and *notch 2* have cardiac, liver and kidney defects. This non-allelic non-complementation of mutant *jagged 1* and *notch 2* alleles has been attributed to either gene dosage or poison models (McCright et al., 2002). The latter posits that in compound mutants, one of the affected gene loci encodes an altered protein that impairs the function of the protein product of the other locus. The study of McCright (McCright, 2002) could not distinguish between these two mechanisms. Our data indicate a role for gene dosage. Although the *notch 2* morpholino used for this study produces altered *notch 2* transcripts (see Materials and methods), and therefore may be interfering with *jagged 2* function through a poison interaction with the zebrafish *jagged 2* ligand, the *notch 5* morpholino, which overlaps the 5′ ATG of the *notch 5* transcript, should not produce an altered gene product. For this reason, we believe reduced gene dosage best accounts for altered biliary development in compound *jagged*/*notch* morphants.

A second aspect of biliary development that may have been revealed by our study concerns the identity of the cell supplying the Notch signal. Although this must be considered to be speculative at this time, we believe our data are consistent with mammalian tissue recombination experiments that suggest that mesenchymal cells signal hepatoblasts to adopt a biliary fate (Shiojiri and Koike, 1997). Supporting this hypothesis, we identified a normal pattern of bile ducts in *cloche* mutants that lack endothelial cells but retain mesenchymal cells that express smooth muscle markers adjacent to developing biliary cells (K.L. and M.P., unpublished). Confirmation of a role for such cells awaits the development of reagents to localize Jagged and Notch proteins in the developing liver.

Finally, results for this study point to a relationship between Notch signaling and other transcriptional regulators of vertebrate biliary development. Studies in the zebrafish (Matthews et al., 2004) and the mouse (Clotmann et al., 2002; Connifer et al., 2002) have shown that the *hnf6* and *hnf1b* genes regulate intrahepatic biliary development as part of a common genetic pathway. Here, we show that *hnf6* gene transcription is reduced 50% in *jagged 2*/*3* morphants, when compared with controls. This suggests that *hnf6*-mediated signaling functions downstream of the Notch signal. However, injection of *hnf6* mRNA does not rescue Notch-deficient morphant larvae. We propose that this is because *hnf6* regulates biliary progenitors whose development is dependent upon the Notch signal.

We thank Jennifer Morrissette and Nancy Spinner for human Jagged 1 constructs. We thank Bruce Appel and Steve Leach for generously providing transgenic fish. This work was supported by grants from the NIH (DK60369 to M.P.) and the Biesecker Family Pediatric Liver Research Center at the Children's Hospital of Philadelphia (M.P.).

Supplementary material

Supplementary material for this article is available at
http://dev.biologists.org/cgi/content/full/131/22/5753/DC1

Note added in proof

Recently, the nomenclature of *jagged* genes has been modified; *jagged 1* is now referred to as *jagged 1a* and *jagged 3* is now referred to as *jagged 1b*.

References

Apelqvist, A., Li, H., Sommer, L., Beatus, P., Anderson, D. J., Honjo, T., Hrabe de Angelis, M., Lendahl, U. and Edlund, H. (1999). Notch signaling controls pancreatic cell differentiation. *Nature* **400**, 877-881.

Appel, B., Givan, L. A. and Eisen, J. S. (2001). Delta-Notch signaling and lateral inhibition in zebrafish spinal cord development. *BMC Dev. Biol.* **1**, 13.

Bierkamp, C. and Campos-Ortega, J. A. (1993). A zebrafish homologue of the Drosophila neurogenic gene Notch and its pattern of transcription during early embryogenesis. *Mech. Dev.* **43**, 87-100.

Chong, S. K., Lindridge, J., Moniz, C. and Mowat, A. P. (1989). Exocrine pancreatic insufficiency in syndromic paucity of the interlobular bile ducts. *J. Pediatr. Gastroenterol. Nutr.* **9**, 445-449.

Clotman, F., Lannoy, V. J., Reber, M., Cereghini, S., Cassiman, D., Jacquemin, P., Roskams, T., Rousseau, G. G. and Lemaigre, F. P. (2002). The onecut transcription factor HNF6 is required for normal development of the biliary tract. *Development* **129**, 1819-1828.

Coffinier, C., Gresh, L., Fiette, L., Tronche, F., Schütz, G., Babinet, C., Pontoglio, M., Yaniv, M. and Barra, J. (2002). Bile system morphogenesis defects and liver dysfunction upon targeted deletion of hnf1beta. *Development* **129**, 1829-1838.

Cornell, R. A. and Eisen, J. S. (2002). Delta/Notch signaling promotes formation of zebrafish neural crest by repressing Neurogenin 1 function. *Development* **129**, 2639-2648.

Dorsky, R. I., Itoh, M., Moon, R. T. and Chitnis, A. (2003). Two tcf3 genes cooperate to pattern the zebrafish brain. *Development* **130**, 1937-1947.

Elmslie, F. V., Vivian, A. J., Gardiner, H., Hall, C., Mowat, A. P. and Winter, R. M. (1995). Alagille syndrome: family studies. *J. Med. Genet.* **32**, 264-268.

Emerick, K. M., Rand, E. B., Goldmuntz, E., Krantz, I. D., Spinner, N. B. and Piccoli, D. A. (1999). Features of Alagille syndrome in 92 patients: frequency and relation to prognosis. *Hepatology* **29**, 822-829.

Field, H. A., Ober, E. A., Roeser, T. and Stainier, D. Y. (2003). Formation of the digestive system in zebrafish. I. Liver morphogenesis. *Dev. Biol.* **253**, 279-290.

Hamada, Y., Kadokawa, Y., Okabe, M., Ikawa, M., Coleman, J. R. and Tsujimoto, Y. (1999). Mutation in ankyrin repeats of the mouse Notch2 gene induces early embryonic lethality. *Development* **126**, 3415-3424.

Henry, C. A., Urban, M. K., Dill, K. K., Merlie, J. P., Page, M. F., Kimmel, C. B. and Amacher, S. L. (2002). Two linked hairy/Enhancer of split-related zebrafish genes, her1 and her7, function together to refine alternating somite boundaries. *Development* **129**, 3693-3704.

Hinton, D. E. and Couch, J. A. (1998). Architectural pattern, tissue and cellular morphology in livers of fishes: relationship to experimentally-induced neoplastic responses. *EXS* **86**, 141-164.

Itoh, M., Kim, C. H., Palardy, G., Oda, T., Jiang, Y. J., Maust, D., Yeo, S. Y., Lorick, K., Wright, G. J., Ariza-McNaughton, L. et al. (2003). Mind bomb is a ubiquitin ligase that is essential for efficient activation of Notch signaling by Delta. *Dev. Cell* **4**, 67-82.

Kamath, B. M., Loomes, K. M., Oakey, R. J., Emerick, K. E., Conversano, T., Spinner, N. B., Piccoli, D. A. and Krantz, I. D. (2002a). Facial features in Alagille syndrome: specific or cholestasis facies? *Am. J. Med. Genet.* **112**, 163-170.

Kamath, B. M., Krantz, I. D., Spinner, N. B., Heubi, J. E. and Piccoli, D. A. (2002b). Monozygotic twins with a severe form of Alagille syndrome and phenotypic discordance. *Am. J. Med. Genet.* **112**, 194-197.

Kortschak, R. D., Tamme, R. and Lardelli, M. (2001). Evolutionary analysis of vertebrate Notch genes. *Dev. Genes Evol.* **211**, 350-354.

Krantz, I. D., Piccoli, D. A. and Spinner, N. B. (1997). Alagille syndrome. *J. Med. Genet.* **34**, 152-157.

Lawson, N. D., Scheer, N., Pham, V. N., Kim, C. H., Chitnis, A. B., Campos-Ortega, J. A. and Weinstein, B. M. (2001). Notch signaling is required for arterial-venous differentiation during embryonic vascular development. *Development* **128**, 3675-3683.

Lekven, A. C., Buckles, G. R., Kostakis, N. and Moon, R. T. (2003). Wnt1 and wnt10b function redundantly at the zebrafish midbrain-hindbrain boundary. *Dev. Biol.* **254**, 172-187.

Lemaigre, F. P. (2003). Development of the biliary tract. *Mech. Dev.* **120**, 81-87.

Lewis, J. (1998). Notch signaling and the control of cell fate choices in vertebrates. *Semin. Cell Dev. Biol.* **9**, 583-589.

Li, L., Krantz, I. D., Deng, Y., Genin, A., Banta, A. B., Collins, C. C., Qi, M., Trask, B. J., Kuo, W. L., Cochran, J. et al. (1997). Alagille syndrome is caused by mutations in human Jagged1, which encodes a ligand for Notch1. *Nat. Genet.* **16**, 243-251.

Liao, W., Bisgrove, B. W., Sawyer, H., Hug, B., Bell, B., Peters, K., Grunwald, D. and Stainier, D. Y. R. (1997). The zebrafish gene *cloche* acts upstream of a *flk-1* homologue to regulate endothelial differentiation. *Development* **124**, 381-389.

Loomes, K. M., Taichman, D. B., Glover, C. L., Williams, P. T., Markowitz, J. E., Piccoli, D. A., Baldwin, H. S. and Oakey, R. J. (2002). Characterization of Notch receptor expression in the developing mammalian heart and liver. *Am. J. Med. Genet.* **112**, 181-189.

Louis, A. A., van Eyken, P., Haber, B. A., Hicks, C., Weinmaster, G., Taub, R. and Rand, E. B. (1999). Hepatic jagged1 expression studies. *Hepatology* **30**, 1269-1275.

Lu, F., Morrissette, J. J. D. and Spinner, N. B. (2003). Conditional *JAG1* mutation shows that the developing heart is more sensitive than the developing liver to JAG1 dosage. *Am. J. Hum. Genet.* **72**, 1065-1070.

Matthews, R. P., Lorent, K., Russo, P. and Pack, M. (2004). The zebrafish onecut gene hnf-6 functions in an evolutionary conserved genetic pathway that regulates vertebrate biliary development. *Dev. Biol.* **274**, 245-259.

McCright, B., Gao, X., Shen, L., Lozier, J., Lan, Y., Maguire, M., Herzlinger, D., Weinmaster, G., Jiang, R. and Gridley, T. (2001). Defects in development of the kidney, heart and eye vasculature in mice homozygous for a hypomorphic Notch2 mutation. *Development* **128**, 491-502.

McCright, B., Lozier, J. and Gridley, T. (2002). A mouse model of Alagille syndrome: Notch2 as a genetic modifier of Jagged1 haploinsufficiency. *Development* **129**, 1075-1082.

McElhinney, D. B., Krantz, I. D., Bason, L., Piccoli, D. A., Emerick, K. M., Spinner, N. B. and Goldmuntz, E. (2002). Analysis of cardiovascular phenotype and genotype-phenotype correlation in individuals with a JAGGED1 mutation and/or Alagille syndrome. *Circulation* **106**, 2567-2574.

McKiernan, P. J. (2002). Neonatal cholestasis. *Semin. Neonatol.* **7**, 153-165.

Norgaard, G. A., Jensen, J. N. and Jensen, J. (2003). FGF10 signaling maintains the pancreatic progenitor cell state revealing a novel role of Notch in organ development. *Dev. Biol.* **264**, 323-338.

Oda, T., Elkahloun, A. G., Pike, B. L., Okajima, K., Krantz, I. D., Genin, A., Piccoli, D. A., Meltzer, P. S., Spinner, N. B., Collins, F. S. et al. (1997). Mutations in the human Jagged1 gene are responsible for Alagille syndrome. *Nat. Genet.* **16**, 235-242.

Pack, M., Solnica-Krezel, L., Malicki, J., Neuhauss, S. C., Schier, A. F., Stemple, D. L., Driever, W. and Fishman, M. C. (1996). Mutations affecting development of zebrafish digestive organs. *Development* **123**, 321-328.

Pandol, S. J. (1998). Pancreatic physiology and secretory testing. In *Sleisenger & Fordtran's Gastrointestinal and Liver Disease*, 6th edn (ed. M. Feldman, W. O. Tschumy, Jr, L. S. Friedman and M. H. Sleisenger), pp. 871-880. Philadelphia, PA: W. B. Saunders.

Piccoli, D. A. and Spinner, N. B. (2001). Alagille syndrome and the Jagged1 gene. *Semin. Liver Dis.* **21**, 525-534.

Piccoli, D. and Witzleben, C. L. (2000). Disorders of the Biliary Tract: Intrahepatic Bile Ducts. In *Pediatric Gastrointestinal Disease* (ed. W. A. Walker, P. R. Durie, J. R. Hamilton, J. A. Walker-Smith and J. B. Watkins), pp. 895-914. Philadelphia, PA: B. C. Decker.

Rogler, L. E. (1997). Selective bipotential differentiation of mouse embryonic hepatoblasts in vitro. *Am. J. Pathol.* **150**, 591-602.

Scheer, N., Riedl, I., Warren, J. T., Kuwada, J. Y. and Campos-Ortega, J.

A. (2002). A quantitative analysis of the kinetics of Gal4 activator and effector gene expression in the zebrafish. *Mech. Dev.* **112**, 9-14.
Shiojiri, N. (1984). The origin of intrahepatic bile duct cells in the mouse. *J. Embryol. Exp. Morphol.* **79**, 25-39.
Shiojiri, N. and Koike, T. (1997). Differentiation of biliary epithelial cells from the mouse hepatic endodermal cells cultured in vitro. *Tohoku J. Exp. Med.* **181**, 1-8.
Shiojiri, N., Inujima, S., Ishikawa, K., Terada, K. and Mori, M. (2001). Cell lineage analysis during liver development using the spf(ash)-heterozygous mouse. *Lab. Invest.* **81**, 17-25.
Spinner, N. B., Colliton, R. P., Crosnier, C., Krantz, I. D., Hadchouel, M. and Meunier-Rotival, M. (2001). Jagged1 mutations in Alagille syndrome. *Hum. Mutat.* **17**, 18-33.
Stainier, D. Y. R., Weinstein, B. M., Detrich, H. W., III, Zon, L. I. and Fishman, M. C. (1995). Cloche, an early acting zebrafish gene, is required by both the endothelial and hematopoietic lineages. *Development* **121**, 3141-3150.
Tanuma, Y. (1980). Electron microscope observations on the intrahepatocytic bile canalicules and sequent bile ducts in the crucian, Carassius carassius. *Arch. Histol. Jpn.* **43**, 1-21.
Taylor, J. S., Braasch, I., Frickey, T., Meyer, A. and van de Peer, Y. (2003). Genome duplication, a trait shared by 22000 species of ray-finned fish. *Genome Res.* **13**, 382-390.
Timmerman, L. A., Grego-Bessa, J., Raya, A., Bertran, E., Perez-Pomares, J. M., Juan-Diez, J., Aranda, S., Palomo, S., McCormick, F., Izpisua-Belmonte, J. C. et al. (2004). Notch promotes epithelial-mesenchymal transition during cardiac development and oncogenic transformation. *Genes Dev.* **18**, 99-115.
Wallace, K. N. and Pack, M. (2003). Unique and conserved aspects of gut development in zebrafish. *Dev. Biol.* **255**, 12-29.
Wanless, I. R. (2002). Anatomy, Histology, Embryology and Development Anomalies of the Liver. In *Sleisenger & Fordtran's Gastrointestinal and Liver Disease* (ed. M. Feldman, W. O. Tschumy, Jr, L. S. Friedman and M. H. Sleisenger), pp. 1195-1201. Philadelphia, PA: W. B. Saunders.
Xue, Y., Gao, X., Lindsell, C. E., Norton, C. R., Chang, B., Hicks, C., Gendron-Maguire, M., Rand, E. B., Weinmaster, G. and Gridley, T. (1999). Embryonic lethality and vascular defects in mice lacking the Notch ligand Jagged1. *Hum. Mol. Genet.* **8**, 723-730.
Yamamoto, T. (1964). Observations on the fine structure of the intrahepatic biliary passages in goldfish (Carassius Auratus). *Z. Zellforsch.* **65**, 319-330.
Zaret, K. S. (2002). Regulatory phases of early liver development: paradigms of organogenesis. *Nat. Rev. Genet.* **3**, 499-512.

Table S1. Cardiac edema in *jagged 2/3* morphants, with and without co-injection of human *Jagged 1* mRNA

Morphants	Cardiac edema	No cardiac edema
J2+3 (*n*=144)	127 (88%)	17 (12%)
J2+3 + human J1 mRNA (*n*=33)	4 (12%)	29 (88%)

Table S2. Phenotypic abnormalities in *jagged*, *notch*, and compound *jagged* and *jagged/notch* morphant larvae

Morphant	Biliary	Cardiac edema	Pancreas	Kidney	CF	Small ears
J1	–	–	–	NA	–	+
J2	+	+*	+*	NA	–	–
J3	–	–	–	NA	+	+
J1+2	+	+	–	NA	–	+
J1+3	–	–	–	NA	+	+
J2+3	+	+	+	+	+	+
N2	–	–	–	NA	–	–
N5	+	+	–	NA	–	–
N2+5	+	+	+	+	–	–
J2+N2	+	+	+	NA	–	–
J2+N5	+	+	+	NA	–	–
J3+N2	–	+	–	NA	+	+
J3+N5	+	+	+	NA	+	+

+, indicated phenotype present in 80-100% of injected 5-dpf larvae.
–, indicated phenotype present in 0-5% of injected 5-dpf larvae.
NA, larvae not analyzed for indicated phenotype.
CF, craniofacial defects.
*Present only in morphants injected with high doses of morpholino.